Scilight

Thermal Science and Applications

https://www.sciltp.com/journals/tsa



Article

Check for updates

Experimental Investigation of Convective Heat-Transfer Performance of Graphite and SiO_2-Graphite Nanofluids for Automotive Radiator Applications

Luke O. Ajuka [1,*] and Peter O. Akindele [2]

[1] Department of Automotive Engineering, University of Ibadan, Ibadan 200005, Nigeria
[2] Department of Mechanical Engineering, University of Ibadan, Ibadan 200005, Nigeria
* Correspondence: ajukamario@gmail.com

How To Cite: Ajuka, L.O.; Akindele, P.O. Experimental Investigation of Convective Heat-Transfer Performance of Graphite and SiO_2-Graphite Nanofluids for Automotive Radiator Applications. *Thermal Science and Applications* **2026**, *1*(4), 372–388. https://doi.org/10.53941/tsa.2026.100023

Received: 13 August 2026
Revised: 16 September 2026
Accepted: 2 October 2026
Published: 5 November 2026

Abstract: Efficient heat transfers in radiators are vital for the life of the engine, to avoid being overheated. Conventional fluids are inefficient in engine cooling, and alternate solutions to prolong engine life must capture enhanced heat transfer, including the application of nanofluids. Despite growing interest in nanofluid-based radiator cooling, limited studies have quantified the comparative performance of base fluids, Gr/Water-EG single nanofluid and SiO_2-Gr/Water-EG hybrid nanofluids under varying concentrations, individually. This study experimentally examined their thermophysical and convective heat-transfer behaviour in a radiator channel flow using thermal conductivity, viscosity, inlet temperature, Nusselt number and Reynolds number as performance indicators. Increasing nanoparticle volumetric fraction enhanced the thermal conductivity of both graphite and SiO_2-Gr nanofluids, whereas increasing ethylene glycol (EG) fraction in the Water-EG base fluid reduced thermal conductivity. Viscosity also increased with volumetric fraction for all fluids, confirming the concentration-induced trade-off between heat-transfer enhancement and flow resistance. The Nusselt number increased with inlet temperature for the Water-EG base fluid and graphite nanofluid, indicating improved convective heat-transfer response at elevated temperature. Conversely, the SiO_2-Gr composite nanofluid showed a reduction in Nusselt number with increasing inlet temperature, suggesting temperature-sensitive transport behaviour; however, at 51 °C, its Nusselt number remained approximately 26% higher than Gr/Water-EG. Reynolds number increased with inlet temperature for the base fluid and graphite nanofluid, indicating stronger inertial flow. Although the hybrid SiO_2-graphite nanofluid exhibited higher Reynolds numbers than the graphite nanofluid under the tested conditions, the observed reduction in Nusselt number with increasing inlet temperature suggests that the thermal enhancement mechanism may be influenced by alterations in fluid properties and particle interactions. Nevertheless, the SiO_2-Gr nanofluid maintained a Reynolds number 66.7% higher than Gr/Water-EG at 51 °C. Overall, the hybrid nanofluid improved heat-transfer performance, although viscosity and flow penalties require optimization for radiators in automotive application.

Keywords: radiator cooling; hybrid nano-fluids; channel flow; convective heat transfer; automotive application; SiO_2-graphite nanofluid

Copyright: © 2026 by the authors. This is an open access article under the terms and conditions of the Creative Commons Attribution (CC BY) license (https://creativecommons.org/licenses/by/4.0/).
Publisher's Note: Scilight stays neutral with regard to jurisdictional claims in published maps and institutional affiliations.

1. Introduction

Heat transfer associated challenges in thermal systems fields, such as automotive (engine cooling), HVAC (refrigeration and air-conditioning heat exchangers), and mechatronics (Heat channels and electronic circuit cooling) are currently experiencing swift revolution through the suspension of nanoparticles in basefluid for their thermal transport assessment [1–3]. For a typical engine, it is known that the use of water as fluids has limitations, such as the potential to freeze at low temperature (32 °F), and to cause duct corrosion when contaminated water is utilized, thereby affecting the water pump [4]. Meanwhile the utilization of pure ethylene glycol (EG) has been reported to carry heat away with 15% less efficiency due to its high viscosity when compared to water, which can result in engine overheating [5].

The problem is that as heat becomes generated in an automotive engine from the process of combustion, with a portion of this heat used to generate power, the remaining heat (surplus) is expected to be expelled as exhaust. If the surplus heat generated is not properly dissipated, it can cause the engine temperature to rise excessively, leading to issues such as overheating, breakdown of lubricating oil viscosity, and wear of engine components. The thermal stress on the engine parts may even result in engine failure. Therefore, it is crucial to have an efficient cooling system in place.

The thermal performance of engine cooling systems can be enhanced through several design, operational, and fluid-based strategies, including increasing the fluid circulation rate [6], enlarging the effective radiator heat transfer surface area [7], optimizing heat exchanger and flow-channel geometries [8,9], promoting fluid-side turbulence, and incorporating additives into conventional working fluids [10,11] or combination of any of these approaches [12]. Although these approaches can improve heat rejection capacity, they are often accompanied by increased pumping power, higher pressure drop, greater system mass, packaging constraints, elevated cost, and additional maintenance requirements [13]. Consequently, improving the intrinsic thermophysical properties of the fluid itself has emerged as a more technically attractive strategy for enhancing engine heat dissipation. In particular, increasing thermal conductivity, preserving adequate specific heat capacity, controlling viscosity, and strengthening convective heat transfer behaviour can improve fluid effectiveness without requiring substantial redesign of the existing cooling architecture [14]. In order to overcome the limitation of the fluids' low thermal conductivity, conventional working fluids are increasingly being blended with nanoparticles to form nanofluids [15].

Therefore, water-ethylene glycol (EG) mixture offers benefits over their individual utilization due to their individual limitations [16], fortunately too, the CFD report by Yaw et al. [1] revealed that adequate heat transfer through additives such as 0.01% hybrid nanofluid, may pave way for miniaturization of an engine. This argument makes it relevant to describe the earlier attempts to improve heat transfer of conventional fluids which were unsuccessful to be due to size of micro-particle used by Maxwell [17], in recent time, however, several studies have indicated that nano-meter sized particles in the host fluid, termed nanofluids can enhance the rate of heat transfer [18].

Nanofluids are liquid suspensions with particles smaller than 100 nm, and having a higher bulk solid thermal conductivity than the base liquid, are currently being utilized to enhance heat transfer in thermal systems [19], by suppressing natural convection [20]. Meanwhile, the radiator is a heat exchanger which removes heat absorbed by fluids, such as water and ethylene glycol, as it passes through the engine block, to cause a controlled temperature of the engine make-up materials in order to avoid mechanical failures due to excessive heat accumulation [21]. Different studies have applied nanoparticles for varying reasons, for example, Sathish et al. [22] examined the thermal performance of aluminium oxide (Al_2O_3) nanoparticles in the applications of solar collector, Shi et al. [23] studied water base aluminium oxide (Al_2O_3) nanofluid to enhance the rate of heat transfer in micro-channel, and Yaw et al. [1] employed the use of graphene nanoplatelets/cellulose nanocrystal for automobile cooling enhancement, while Tumane et al. [24] applied Cu nanoparticle in water base fluid to achieved an to improve the heat transfer performance of a radiator.

Furthermore, based on reports of previous studies (publication trend) on nanofluids, hybrid nanofluids and convective heat-transfer (Figure 1) in radiator cooling, there have been many suggestions that by selectively combining two different types of nanoparticles, the hybrid nanofluid exhibits higher heat transfer rates compared to its individual nanoparticle counterparts [25,26], and this should directly improve heat transfer properties of the basefluid, and positively impact the life of the engine.

Other related studies include that of Arbak et al. [27] which experimentally examined the heat transfer characteristics of bimetallic nanoparticles (CuO–ZnO) in automotive radiators using four different fluids under constant heating power. Two cartridge heaters, each with a power of 160 W, are used to heat the nanofluid within a half (½) inch cross pipe fitting, with the heated nanofluid is then directed to a heat exchanger with a width and height of 120 mm. They noted that an additive ratio of 0.3% gave the highest UA value compared to the 0.1% and

0.2% water-bimetal mixture fluids, and further increase in the bimetallic nanoparticle additive rate generated a corresponding increase in heat transfer rate. Additionally, Ukueje et al. [28] conducted a comprehensive review to provide an overview of the thermal conductivity of hybrid nanofluids and their potential application in cooling automobile radiators. They noted that hybrid nanofluids have better thermal conductivity and heat transfer coefficient than mono nanofluids and regular liquids, possibility of obtaining optimum thermal augmentation at lowest concentrations (approximately less than 0.1 vol. %) based on the uniformity of dispersion process. They concluded that automobile radiator's overall heat transfer can be enhanced using a mixture of nanofluids as conventional fluids, because one nanoparticle acts as the core while the others adhere to the core, resulting in enhanced thermal conductivity. Furthermore, Cardenas Contreras and Bandarra Filho, [29] studied the heat transfer performance of an automotive radiator using MWCNT nanofluid dispersed in a binary mixture of water-EG (50:50) within a wide range of high operating temperatures. At 0.025%, 0.05% and 0.1% volume fractions using the two-step method of synthesis, the nanoparticle concentration and fluid inlet temperature impact were evaluated for corresponding heat transfer rate and the overall heat transfer coefficient. Using a constant 2 m/s air velocity and 0.09 kg/s to 0.11 kg/fluid mass flow rate, 4.6% and 4.4% heat transfer rate and overall heat transfer coefficient were obtained, respectively. They concluded that an increase in concentration increases heat transfer performance, however, at high nanofluid inlet temperatures, performance decreases. In addition, Ramji et al. [30] investigated the use of Tungsten Trioxide (WO_3) Nano-fluid in an automotive radiator. The study utilized H_2O-WO_3 as operational fluid and compared the heat transfer rate and outlet temperature of fluid for various flow rate which ranged from 0.2 m^3/hr to 0.5 m^3/hr. At a frequency of 30 kHz and 1000 watts power, the nanofluid was ultrasonicated for 4 h to prepare three samples with 0.0166%, 0.0334%, and 0.06667% volume concentrations. Based on experiments and having set the inlet condition of fluid was set at 50 °C, with a reported minimal temperature variation in the system, they reported a 4.18% maximum increase in the heat transfer rate compared to the basefluid.

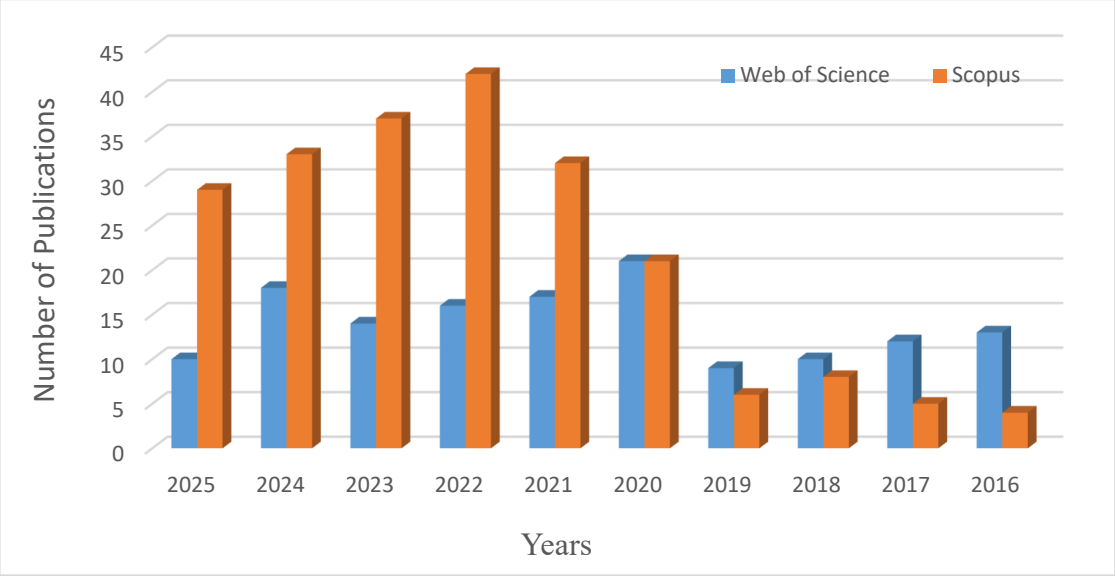


Figure 1. Comparative annual distribution of publications for studies related to nano-fluids, hybrid nanofluids and convective heat-transfer performance (Source: Scopus & Web of Science, 2016 to 2025).

In another study, Erkan et al. [31] examined the impact of using nanofluids (Al_2O_3, SiO_2, TiO_2) over conventional water, with ethylene glycol, in automotive radiators on the exegetic properties of diesel engines. To ensure a well-blended mixture of nanoparticles and the base fluid, a SONICS Vibra cell magnetic stirrer was utilized at 20 min duration, pulse 10.03, and 60% amplitude. At 1800 rpm fixed engine speed, six different nanofluid tests were performed on two different dispersions rates (0.2% and 0.4%). They noted that in the values of the experimental parameters, pure water lagged behind the nanofluids performance, and the least exhaust temperature value was obtained using Al_2O_3/Ethylene Glycol mixture with an 8.858 kW of exergy exhaust value. And Vele and Patil [32] conducted a review study of heat transfer enhancement in car radiators utilizing nanofluids. They noted that the thermo-physical characteristics (thermal conductivity, viscosity and density) nanofluids are substantially higher than the base liquid. The study focused on the gap related to thermal conductivity and viscosity measurement of fluid mixture. They submitted that nanoparticles concentration and temperature increase thermal conductivity, but viscosity and density decreased with temperature and increases with nanoparticles concentration.

The authors further recommended that more studies should be conducted to get a better comprehension of augmentation mechanisms of heat transfer using hybrid nanofluids and its real-life applications.

Furthermore, on other recent study reports, Kanti et al. [33] combined experiments, numerical simulations, empirical correlations, and Bayesian-optimized XGBoost modelling to predict the Nusselt number, friction factor, and entropy generation of 50:50 Al_2O_3-CuO/water hybrid nanofluids under turbulent tube flow. They reported a strong predictive accuracy and up to 71% lower total entropy generation; however, the restricted turbulent-flow geometry and material system limits a direct applicability to automotive radiators operating with graphite-based Water-EG nanofluids. In addition, an earlier study by Ajuka et al. [34] theoretically evaluated the entropy generation in graphene-nanoplatelet nanofluids flowing through micro- and minichannels, and they reported that particle concentration, channel scale, and base-fluid composition strongly govern the competing contributions of thermal and frictional irreversibility; however, the theoretical laminar-flow analysis did not provide radiator-scale experimental validation or data-driven performance prediction. Moreso, the experimentally investigated surfactant-stabilized 50:50 MWCNT-Al_2O_3/water hybrid nanofluids in an outdoor flat-plate solar collector by Kanti et al. [35] demonstrated the application potential of stabilized hybrid suspensions for improving solar-thermal performance; nevertheless, its water-based collector configuration differs substantially from the forced-convection, Water-EG automotive radiator environment considered here and does not constitute a machine-learning modelling study. Here, the present study experimentally compares graphite and SiO_2-graphite nanofluids in a Water-EG coolant under radiator-relevant conditions, with emphasis on concentration-dependent thermophysical behaviour and the balance between convective enhancement and flow-related penalties; the resulting dataset also establishes a basis for subsequent machine-learning-assisted prediction and multi-objective optimization. Therefore, this study is being conducted to provide better insight on the heat transfer performance of hybrid and composite nanofluids for a pragmatic application, experimentally.

2. Nanofluids Concepts, Properties and Applications

Nano-fluids are advanced heat-transfer fluids formed by dispersing nanoscale solid particles, typically metals, metal oxides, carbon-based materials or hybrid nanoparticle systems, into conventional base fluids such as water, ethylene glycol, engine oil or water-ethylene glycol mixtures. The concept was established to overcome the relatively low thermal conductivity of traditional fluids by introducing nanoparticles with superior thermal transport capability into the fluid matrix [36]. Their enhanced performance is generally attributed to improved effective thermal conductivity, Brownian motion, interfacial nanolayer formation, particle-fluid interaction and micro-convective transport mechanisms [37]. However, nanofluid performance is not governed by thermal conductivity alone, since dynamic viscosity, density, specific heat capacity, colloidal stability and pressure drop collectively determine the practical heat-transfer effectiveness of the suspension. Recent reviews have shown that nanofluids can improve convective heat-transfer coefficients substantially, but viscosity rise and stability degradation remain major limitations for long-term deployment in engineering systems [38]. Consequently, nanofluids are increasingly applied in automotive radiators, microelectronics cooling, heat exchangers, solar thermal systems, photovoltaic-thermal collectors and industrial thermal-management systems where compactness, high heat removal rate and energy efficiency are required.

2.1. Factors Affecting Nano-fluid Performance and Convective Heat Transfer Characteristics

The performance of a nanofluid is controlled by nanoparticle concentration, particle size, morphology, material composition, base-fluid chemistry, temperature, pH, surfactant dosage, sonication time and flow regime. Increasing nanoparticle volume fraction generally improves thermal conductivity and Nusselt number because more thermally conductive solid pathways are introduced into the base fluid, but excessive loading may increase viscosity, intensify particle agglomeration and raise pumping power requirements [37]. Temperature also plays a critical role, since higher temperature can enhance Brownian motion and reduce base-fluid viscosity, thereby improving convective transport, although poor suspension stability at elevated temperature may reduce performance reliability. In forced convection, Reynolds number, Prandtl number and Nusselt number are key descriptors of heat-transfer behaviour, with higher Reynolds number typically promoting turbulence, thinner thermal boundary layers and improved convective heat transfer. For radiator and heat-exchanger applications, the best nanofluid formulation is therefore not the one with maximum nanoparticle loading, but the one that provides an optimum balance between heat-transfer enhancement, viscosity penalty, pressure drop, stability and thermal efficiency. This performance compromise explains why current studies increasingly focus on hybrid nanofluids, optimized mixture ratios and machine-learning-assisted property prediction to maximize heat transfer while minimizing hydraulic losses [38,39].

2.2. Review of Hybrid Nanofluids Application in Radiators

Hybrid nanofluids have received increasing attention in radiator cooling because the combination of two or more nanoparticle classes can provide complementary thermal, structural and rheological advantages beyond those obtainable from mono nanofluids. In automotive radiators, oxide, metallic and carbon-based nanoparticle systems have been shown to improve convective heat transfer coefficient, Nusselt number, fluid temperature drop and overall heat rejection relative to conventional water or water-glycol fluids. Early radiator studies demonstrated that TiO_2/water and TiO_2/ethylene-glycol-water nanofluids enhanced convective heat transfer by about 20–37%, confirming the sensitivity of radiator performance to nanoparticle loading, Reynolds number and base-fluid composition [10]. Graphene and graphene-oxide-based fluids further extended this performance envelope, with reported improvements in overall heat transfer coefficient and radiator effectiveness arising from the high thermal conductivity and two-dimensional heat-spreading capacity of carbon nanostructures [40,41]. A major transition in the literature is the shift from mono nanofluids to hybrid systems, as Abbas et al. [42] reported that Fe_2O_3-TiO_2/water hybrid nanofluid improved heat transfer rate and Nusselt number by 26.7% and 20.03%, respectively, at low concentration, although excessive loading reduced performance due to stability and blockage effects. Similarly, Li et al. [43] showed that SiC-MWCNT hybrid nanofluids produced a 26.5% improvement in convective heat-transfer coefficient compared with pure ethylene glycol, while Kumar et al. [44] reported about 40% enhancement in temperature drop and cooling capacity using MWCNT-SiO_2/ethylene glycol-water hybrid nanofluid in a louvered fin radiator.

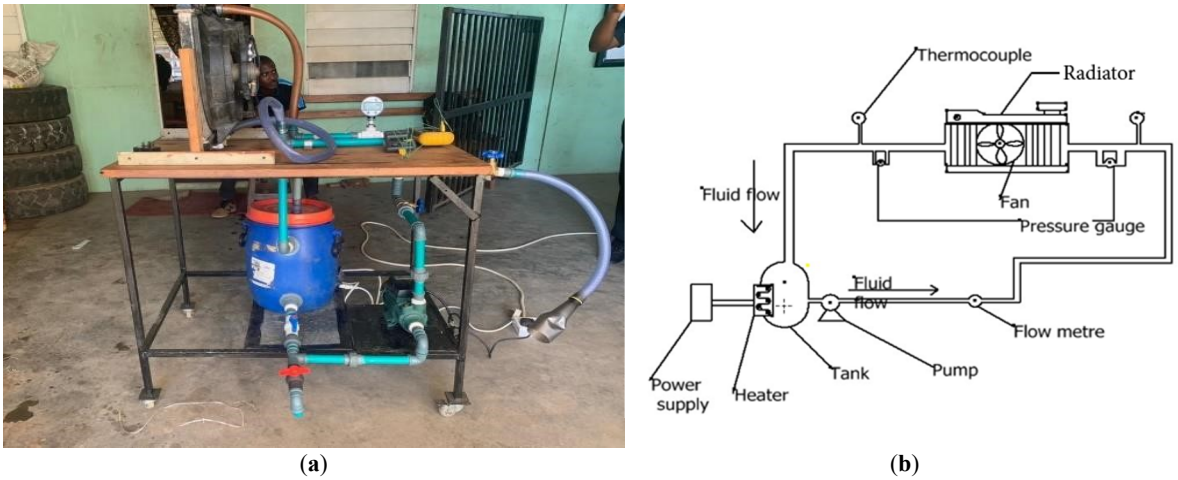
Recent experimental radiator investigations have strengthened the evidence that hybridization can improve thermal performance but also introduces hydraulic penalties. Hassaan [45] experimentally tested MWCNT-Al_2O_3/water hybrid nanofluid in an automobile radiator and reported increases of 28.5% in convection heat-transfer coefficient, 22.54% in effectiveness and 23.74% in Nusselt number, but with pressure-drop increments of up to 24%, indicating the unavoidable trade-off between heat-transfer enhancement and pumping power. Numerical and simulation-based studies have also examined Al_2O_3, CuO and Al_2O_3-CuO hybrid nanofluids in water and ethylene-glycol-water mixtures, showing that heat-transfer coefficient increases with Reynolds number and nanoparticle concentration, but that mixture ratio, dispersion stability, interparticle interaction and base-fluid selection must be optimized before hybrid nanofluids can be reliably deployed in radiators [46]. More recently, ternary hybrid nanofluids have been investigated for ruffled-fin automotive radiators, with Fe/Cu/Ag, Fe/Cu/ZnO and Ag/Al_2O_3/TiO_2 combinations improving Nusselt number and overall heat-transfer coefficient, while an optimum case produced a 44.6% outlet-temperature reduction; however, the performance index decreased by 5.8–11.7%, confirming that thermal enhancement must be assessed together with hydraulic and efficiency penalties (Oshionebo et al., 2025) [12]. Collectively, these studies establish hybrid nanofluids as promising radiator fluids, but their practical adoption remains constrained by viscosity rise, sedimentation, agglomeration, corrosion risk, material compatibility, cost, repeatability and limited long-duration engine-cycle validation.

The reviewed literature shows a consistent performance pattern; nanoparticle addition generally improves thermal conductivity and Nusselt number, but at the expense of increased viscosity, pressure drop and pumping power, making thermo-hydraulic optimization more important than thermal enhancement alone. The major research goal addressed in this study is the limited availability of coupled thermophysical and convective-performance data for graphite and SiO_2-graphite/Water-EG nanofluids under concentration-dependent radiator-relevant conditions. While previous studies have reported enhancements for TiO_2, Al_2O_3, CuO, Fe_2O_3-TiO_2, MWCNT-Al_2O_3, SiC-MWCNT and ternary nanofluids, fewer studies have systematically linked concentration, mixture-ratio effect, viscosity penalty, Nu-Re dependence and THPI for SiO_2-graphite hybrid nanofluids. Therefore, the present study contributes by clarifying whether the hybrid SiO_2-graphite formulation provides a net thermal advantage over graphite-only nanofluid when both heat-transfer enhancement and hydraulic resistance are considered.

3. Materials and Methods

In this study, two different nanoparticles, SiO_2 (5–20 nm, 99.5%, white) and Graphite (25–60 nm, black) powders (Sigma-Aldrich, St. Louis, MO, USA) were commercially sought, and the manufacturer specifications adopted. The steps involved in this experimental study using Water-ethylene glycol (W/EG) based graphite, silicon IV oxide (SiO_2), and graphite-silicon IV oxide (Gr-SiO_2) nanofluids at different volume fractions are well detailed in this section. For stability and elimination of particle agglomeration, the nanofluid (suspension) was magnetically stirred for 12 h at 600 rpm and subsequently ultrasonicated for 60 min under continuous operation using a Branson M2800H ultrasonic bath operating at a nominal frequency of 40 kHz. The sample was contained in a sealed vessel and indirectly immersed in the bath, while the bath temperature was monitored and maintained below 30 °C to minimize temperature-induced property changes, and the suspension was observed to be visually homogeneous at

the time of testing. In addition, thermal conductivity was estimated over the investigated temperature range of 25–60 °C using the stated effective-property mixture model and the constituent thermal conductivities, while dynamic viscosity was measured at the corresponding test temperatures using an Anton Paar (MCR 303) modular compact rotational rheometer equipped with a concentric-cylinder measuring geometry and a Peltier cylinder temperature-control system, selected to provide adequate sensitivity and controlled shear conditions for low-viscosity water–ethylene glycol nanofluids. Measurements were conducted over a shear-rate range of 10–1000 s^{-1} after thermal equilibration at each test temperature. Dynamic viscosity was determined from the shear-independent region of the flow curve. Three measurements were performed for each sample, and the results were reported as the mean and standard deviation. The rheometer provides a nominal torque range of 1 nN·m to 230 mN·m. The experimental rig set-up with the measurement instrumentations is shown in Figure 2 a,b. The rig includes a tank, pump, radiator, connecting tubes and measurement devices (thermocouples, pressure gauges, a flow-meter, etc.) and other accessories (valves, a cross flow finned heat exchanger (radiator), a cooling fan, and a storage tank (with an embedment of a heater coil connected to heating source to raise the temperature of the working fluid).



(**a**) (**b**)

Figure 2. (**a**): Front and side views of experimental set-up; (**b**): Schematic view of experimental set-up.

The inlet and outlet temperatures and pressures of the fluid were measured using thermocouples and pressure gauges, while fluid flow rate was determined by an Omega FL-45100, with 100 °C temperature limit flow meter (see Tables 1–3) for specific details of measuring devices, test rig, and pump specification) and Table 4 for material features. For the baseline control experiment, 5 L of distilled water was charged into the test reservoir without the addition of nanoparticles, and all relevant experimental parameters were measured and recorded under identical operating conditions. This configuration served as the reference case for evaluating the influence of nanoparticle incorporation on the thermophysical and heat transfer performance of the working fluid. The experimental procedure was subsequently repeated using a different mixture ratio of water-to-ethylene glycol (Water-EG) base-fluid mixture without nanoparticle addition. All operating conditions, measurement protocols, and data acquisition procedures were maintained constant to ensure experimental consistency and enable direct comparison with the distilled water control. The nanoparticle-free water-EG mixture constituted a secondary benchmark for assessing the performance enhancements attributable solely to nanoparticle dispersion.

Thereafter, nanofluids containing varying concentrations of graphite (Gr), silicon dioxide (SiO_2), and hybrid graphite-silicon dioxide (Gr-SiO_2) nanoparticles were prepared using the water-EG basefluid and subjected to experimental evaluation. During each test, the fluid was circulated through the experimental loop, while two gate valves were employed to regulate and maintain the desired flow rate. The corresponding thermal and hydraulic performance parameters were recorded systematically for subsequent analysis and comparison with the control and base-fluid benchmark cases. The specifications of the materials used in the experiment are listed below:

Table 1. Technical specification values of measuring device.

S/N	Measurement Device	Range	Uncertainty
1	Flow Meter	2–40 L/min	±0.17 L/min
2	Thermocouple	0–250 °C	±0.035 °C
3	Pressure Guage	1–280 psi	±0.035 psi

Table 2. Dimensions of radiator heat exchanger (test rig specification).

S/N	Parameter	Value
1	Number of tubes	34
2	Radiator length	371mm
3	Radiator width	527mm
4	Width of the radiator tube	37.5mm
5	Tube Length	355mm
6	Fin Length	9mm
7	Fin thickness	0.08mm
8	Distance between adjacent fins	14mm

Table 3. Pump specification.

S/N	Pump Parameter	Value
1	Maximum Voltage	220 v (A/C)
2	Flow rate	5–35 L/min
3	Frequency	50 Hz
4	Maximum Current	2.1 A
5	Power Rating	0.5 hp

Table 4. Experimental material characteristics.

Experimental Materials		Density	SHC	Particle Size	Viscosity (cP)	Thermal Cond-Uctivity (W/m/K)
Nanoparticles						
	Graphite	1800	706.9	25–60 nm	N/A	129
	SiO_2	2650	680	5–20 nm	N/A	1.4
Basefluids						
	Distilled Water	1000	4181	N/A	0.890 cP @ 25 °C	0.607
	Ethylene Glycol	1115	3140	N/A	18.376 cP @ 20 °C	0.251

Experimental Description

For the nanofluid preparation, water and Water-EG (100, 50:50, 30:70) ratio were utilised. In Figure 2b, the heated (hot) basefluid flows from the reservoir tank to the radiator, while the cooler fluid returns to the reservoir tank. The thermocouples measure the temperature of the fluid at the inlet and the outlet of the car radiator, while the thermostat of the heater regulates the temperature of the fluid. The experiment was conducted by varying the volumetric fraction of the nanoparticles in the nanofluid. The pump is switched off to allow the nanofluid sample inside the tank to heat up and reach the intended temperature of 60 °C. Once this maximum temperature has been reached, the pump is switched on and the nanofluid sample is pumped into the car radiator. The fluid exiting the radiator will flow back to the storage tank and the cycle repeats itself, while the parametric measurements (temperature, pressure, flowrate, etc.) were being recorded throughout this process at a set time interval over a fixed period of 10 mins to determine the fluid flow characteristics.

The volume fraction of hybrid nanofluid was determined by:

$$\emptyset = \frac{{m_{Gr}}/{\rho_{Gr}} + {m_{SiO2}}/{\rho_{SiO2}}}{{m_{Gr}}/{\rho_{Gr}} + {m_{SiO2}}/{\rho_{SiO2}} + {m_{bf}}/{\rho_{bf}}} \tag{1}$$

where ϕ = volume fraction, V_{np1} = volume of graphite nanoparticle, V_{np2} = volume of SiO_2 nanoparticle, V_{bf} = volume of base fluid.

Heat transfer heat in fluid:

$$Q_c = m_c C_{p,c}\left(T_{c,in} - T_{c,out}\right) \tag{2a}$$

$$Q_a = m_a c_{p,a}\left(T_{a,out} - T_{a,in}\right) \tag{2b}$$

Energy-balance ($\in_{EB}$) closure:

$$\in_{EB} = \frac{|Q_c - Q_a|}{{(Q_c + Q_a)}/{2}} \times 100 \tag{2c}$$

Heat-transfer rate evaluation:

$$Q_{avg} = \frac{Q_c + Q_a}{2} \tag{2d}$$

where Q = Heat transfer (W), ρ = density of the fluid (kg/m^3), Cp = specific heat (J/°C·kg), Ti and T_o are inlet and outlet temperatures.

Density for nanofluid:

$$\rho_{nf} = (1-\phi)\rho_{bf} + \phi_{Gr}\rho_{Gr} + \emptyset_{SiO2}\rho_{SiO2} \tag{3}$$

Specific heat capacity of the nanofluid;

$$\mathrm{cp_f} = \frac{\mathrm{p_{wf}}(1-\phi)\mathrm{cp_{wf}}}{\mathrm{p_f}} + \frac{\mathrm{p_{EGf}}\phi}{\mathrm{p_f}}\ \mathrm{cp_{EGf}} \tag{4}$$

where p_{wf}, p_{EGf}, and p_f are the densities of water, ethylene glycol fluid, the water–ethylene glycol mixture, respectively.

Nusselt number (Nu):

$$Nu_{exp} = \frac{h_{exp}D_h}{k_{nf}} \tag{5}$$

$$h_{exp} = \frac{Q_C}{A_S\,(T_{b,m}-T_{w,m})};$$

where $T_{b,m}$ and $T_{w,m}$ are the mean bulk coolant and mean tube-wall temperatures, respectively.
Where h_{exp} = heat transfer coefficient (W/m^2·°C), Q = heat transfer (W), A_s = surface Area.

Hydraulic diameter (D_h):

$$D_{h=}\frac{4A_{tube}}{P_{tube}}; \tag{6}$$

where D_h = Hydraulic diameter (m), A_{tube} = Area of tubes (m^2), P_{tube} = Perimeter of tube (m).

Reynolds Number of fluid (Re):

$$Re_{fluid=}\frac{\rho_{\mathrm{fluid}} * \mathrm{D_h} * \mathrm{v_f}}{\mu\mathrm{f}} \tag{7}$$

where $V_f = \frac{V}{N_t A_t}$; $Re_{fluid} = Reynolds\ Number, p_{fluid=\ Density\ of\ the\ fluid}(\mathrm{kg/m^3})$, V_f = mean fluid velocity within each tube, V = total volumetric flow rate, N_t = Number of tubes carrying flow in parallel.

Thermal Conductivity-to-Viscosity Ratio (Performance Ratio):

$$\frac{k/k_{bf}}{\mu/\mu_{bf}} \tag{8}$$

Thermo-hydraulic performance criterion (PEC):

$$\frac{Nu_{nf}/Nu_{bf}}{(f_{nf}/f_{bf})^{1/3}} \tag{9a}$$

where friction factor '*f*' is the Petukov's correlation determined as;

$$f = (0.79InRe - 1.64)^{-2} \tag{9b}$$

where Nu_{nf}, Nu_{bf}, f_{nf}, and f_{bf} are the Nusselt numbers and friction factors of the nanofluid and basefluid, respectively.

Standard Deviation (SD):

$$SD = \sqrt{\frac{\sum_{i=1}^{3}(x_i - \bar{x})^2}{3-1}} \tag{10}$$

Standard Uncertainty:

$$u_{Qnf} = \left[\sum_{i=1}^{n}\left(\frac{\partial Q_{nf}}{\partial x_i}\right)^2\right]^{1/2} \tag{11}$$

where x_i represents each independently measured input variable.

4. Results and Discussion

At constant inlet temperature (50 °C) and fluid volumetric flow (4×10^{-2} m^3/s), heat characteristic of the nanofluids were determined as shown in Table 5, which reveals the variations in the outlet temperatures and pressures. At smaller concentrations of nanoparticle (Gr and SiO_2), the were decrease in outlet temperatures and increase in pressures as volume fractions increased, while at significant volume fractions, temperatures and pressures increased with increased volume fractions. The Table 5 shows the outcome properties of the addition of graphite, silicon IV oxide, and graphite-silicon IV oxide nanoparticles to water–ethylene glycol (W/EG) of different concentrations. Observation reveals that the density, viscosity and heat transfer of W/EG increased with increase in graphite nanoparticle concentration, and at increased concentrations of Graphite + SiO_2), whereas only the density and heat transfer increased when SiO_2 was added to W/EG, while the specific heat increased but later decreased as concentration increased. This may be attributed to the low heat conduct of silicon IV oxide especially at higher concentration. Meanwhile, observation reveals that addition of silicon IV oxide to W/EG and graphite nanofluid dampened the heat transfer properties of the nanofluid with an increased silicon IV oxide concentration causing a major reduction in this value.

Table 5. Properties of nanofluids at different concentrations at 50 °C and 4×10^{-5} m^3/s of $(n = 3)$ independently repeated runs.

Nanofluid	Vol. Fraction (vol. %)	T_o (°C)	P (Psi)	Density (kg m^{-3})	Viscosity (Pa·s)	C_p (J/Kg°C)	Q_{nf} (W)	UQ_{nf}
Gr/Water-EG	8.714×10^{-3}	48.15 ± 0.18	58.90 ± 0.42	1024.529 ± 1.12	0.011810 ± 0.00012	3503.598 ± 18.42	10,495.863 ± 178.43	162.7
Gr/Water-EG	1.743×10^{-2}	35.50 ± 0.16	92.63 ± 0.61	1024.508 ± 1.06	0.011814 ± 0.00014	3504.469 ± 20.15	19,787.401 ± 316.59	294.8
Gr/Water-EG	2.614×10^{-2}	19.38 ± 0.12	103.25 ± 0.72	1024.846 ± 1.24	0.011817 ± 0.00015	3502.417 ± 21.06	38,262.083 ± 612.19	568.6
SiO_2/Water-EG	3.205×10^{-2}	49.83 ± 0.20	92.63 ± 0.64	1036.873 ± 1.38	0.012020 ± 0.00013	1644.189 ± 11.27	3879.337 ± 73.42	65.3
SiO_2/Water-EG	3.76×10^{-2}	45.02 ± 0.17	89.13 ± 0.58	1064.372 ± 1.51	0.011822 ± 0.00014	1688.932 ± 12.16	6154.491 ± 105.66	96.8
SiO_2/Water-EG	4.388×10^{-2}	43.00 ± 0.19	87.22 ± 0.55	1094.222 ± 1.63	0.011825 ± 0.00015	1661.048 ± 11.84	6773.470 ± 117.24	108.5
Gr-SiO_2/Water-EG	0.0910	44.49 ± 0.18	85.25 ± 0.53	1010.283 ± 1.17	0.01280 ± 0.00016	4005.759 ± 23.45	3262.398 ± 61.34	54.9
W/EG + (Gr + SiO_2)	0.1667	49.29 ± 0.21	99.50 ± 0.69	1018.837 ± 1.29	0.01597 ± 0.00021	3862.704 ± 24.17	3198.690 ± 63.71	56.2
W/EG + (Gr + SiO_2)	0.2160	49.68 ± 0.22	100.00 ± 0.74	1084.408 ± 1.56	0.01843 ± 0.00025	3788.779 ± 25.31	2665.828 ± 55.98	48.6

Where, T_o, V, Cp and Q_{nf} are the inlet temperature, outlet temperature, volumetric flow rate, specific heat and the heat transfer rate of the nanofluids, respectively.

4.1. Validation of Experimental Results Using Established Correlations

The thermal-hydraulic behaviour of Gr/Water-EG and SiO_2-Gr/Water-EG nanofluids were semi-empirically validated, with the experimentally determined Nusselt numbers and friction factors compared with established correlations. The Dittus–Boelter correlation was used for heat-transfer validation, while the Petukhov correlation was used for friction-factor validation (Figure 3). The comparison was performed using the same hydraulic diameter, measured flow conditions, and thermophysical properties evaluated at the bulk mean temperature.

4.2. Thermal Conductivity of Fluid at Different Concentration

The impact of volumetric fraction on the thermal conductivity of Water-EG fluids, Gr/water-EG nanofluids and SiO_2-Gr/Water-EG is shown in Figure 4. Accordingly, observation shows that the thermal conductivity of Water-EG fluids decreases with increasing concentration of EGC while in the case of Gr/Water-EG, the thermal conductivity of the nanofluids increases with increasing volumetric concentration of Graphite nanoparticles. It can be inferred that at varying mixture ratios of Water-EG (100, 50:50, 30:70), a sharp decline in thermal conductivity is evident, indicating that compared to nanofluids, the presence of nanoparticles elevated the heat conduction of the Water-EG. The increase in the volume of EGC in Water-EG does not have a positive impact on the thermal conductivity of the Water-W/EG as fluid. Meanwhile, at different concentrations of the SiO_2-Gr/Water-EG nanofluid, addition of SiO_2 at small concentration does not cause much dampening effect on the thermal conductivity of the nanofluid.

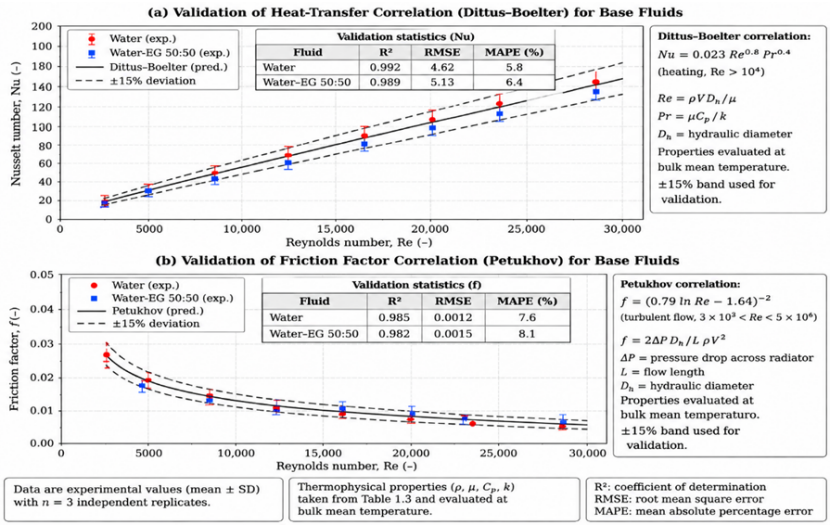


Figure 3. Validation of heat-transfer and friction correlations using base fluids. (**a**) against Dittus-Boelter correlation; (**b**) Petukov correlation.

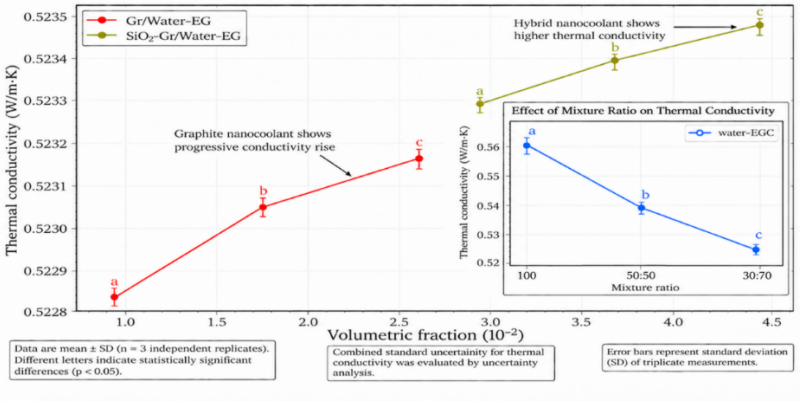


Figure 4. Comparison between thermal conductivity of Water-EG fluids, Graphite/Water-EG nanofluids and SiO_2-Gr/Water-EG.

4.3. Viscosity of Fluids at Different Concentration

The impact of volumetric fraction on the viscosity of Water-EG fluids, Gr/Water-EG nanofluids and SiO_2-Gr/Water-EG is illustrated in Figure 5. In the Figure, the viscosity of Water/EGC fluids increases with increasing concentration of EGC, at different mixture ratio of Water-EG (100, 50:50, 30:70). Moreso, as the volume of nanoparticle concentration increased, viscosities increased for all as volume fractions. The obvious sharp increase in the case of graphite-EGC nanofluid became more evident at 1.743×10^{-2} showing that increase becomes more significant as volume concentration increases. Overall, the results indicate that viscosity remains concentration-dependent, with the hybrid nano-fluid showing a more pronounced viscosity response than the graphite-only suspension.

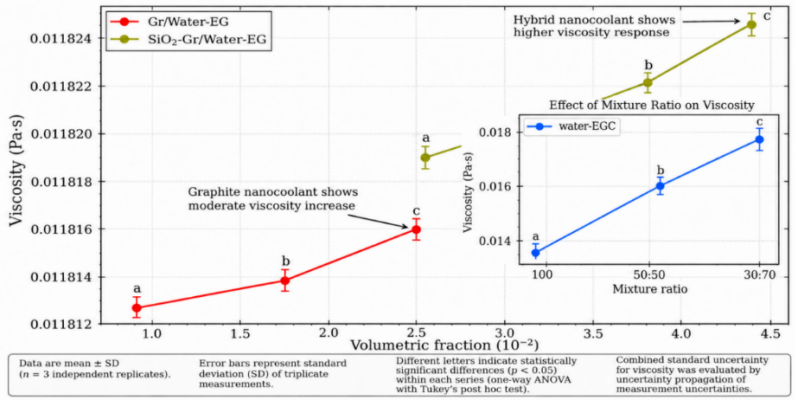


Figure 5. Viscosity of Water-EG, Gr/Water-EG nanofluids and SiO_2-Gr/Water-EG fluids.

4.4. Effect of Fluid Inlet Temperature on the Fluid Side Nusselt Number

The relationship of the inlet temperature with the fluid side Nusselt number of Water-EG fluids, Gr/Water-EG nanofluids and SiO_2-Gr/Water-EG is shown in Figure 6. The Nusselt number for Water/EGC fluids increased with increase in inlet temperature. Likewise for Gr/Water-EG nanofluid, the Nusselt number increased with increase in inlet temperature indicating that heat transfer is more of convection than conduction. Meanwhile, for SiO_2 fortified nanofluid, the Nusselt number decreased with increase in inlet temperature (meaning that more volume of SiO_2 may be needed for better heat transfer by conduction. Although classical forced-convection theory generally predicts increasing heat-transfer coefficients with increasing Reynolds number and temperature-dependent property variations, observed decrease in Nusselt number for the SiO_2-graphite nanofluid with increasing inlet temperature may be associated with concentration-dependent changes in effective viscosity, thermal diffusivity, particle clustering, further validation measurements may be required before a definitive mechanistic explanation. At 51 °C, the SiO_2-Gr/Water-EG nanofluid exhibited an approximately 26% higher Nusselt number than the Gr/Water-EG nanofluid, indicating greater convective heat-transfer performance under the investigated condition.

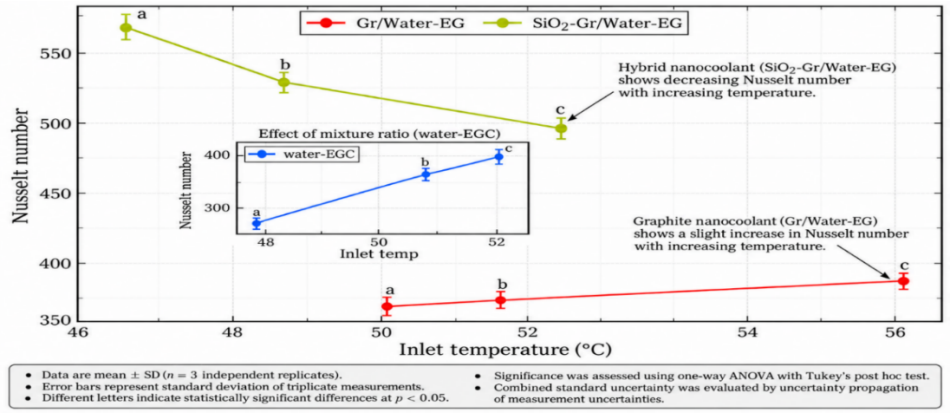


Figure 6. Impact of inlet temperature on the Nu of Water-EG fluids, Gr/Water-EG, & SiO_2-Gr/Water-EG.

4.5. Effect of Fluid Inlet Temperature on the Fluid side Reynolds Number

The relationship of the inlet temperature with the fluid side Reynolds number of Water-EG fluids, Gr/Water-EG nanofluids and SiO_2-Gr/Water-EG is represented in Figure 7. In the Figure, the Reynolds number increased with increase in inlet temperature for Water/EGC and Gr/Water-EG, indicating potential for increased drag coefficient and a decreased lift condition, unlike the case of a decreasing Reynolds number for SiO_2-Gr/Water-EG, which is associated with the increasing inlet temperature. The presence of SiO_2 dampens the conductivity of the nanofluid to foster laminar flow potential, with the composite (SiO_2-Gr/Water-EG) nanofluid having a 66.7% higher Reynolds number than Gr/Water-EG nanofluid at 51 °C.

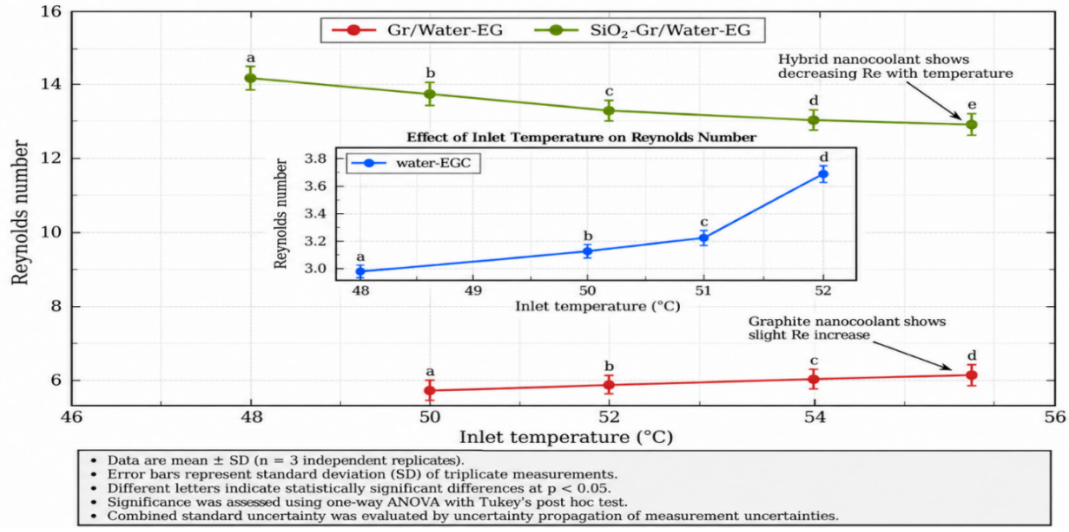


Figure 7. Variation of Re with inlet temperature for Water-EG, Gr/Water-EG, & SiO_2-Gr/Water-EG.

4.6. Effect of Volume Fraction of Nanoparticles on Nusselt Number

The impact of the volume fraction of nanoparticles on Nusselt numbers on Water-EG, Gr/Water-EG and SiO_2-Gr/Water-EG fluids is illustrated in Figure 8. As illustrated in Figure 8, the Nusselt number for Gr/Water-EG decreased as the volume concentration increased, this is an indication that heat transfer is dominated by convection. Nusselt number increased for Water/EGC and SiO_2-Gr/Water-EG as volume concentration increased, indicating that heat transfer is dominated by conduction, and the Nusselt number of SiO_2-Gr/Water-EG surpasses the Nusselt number of Gr/Water-EG by 25.93%.

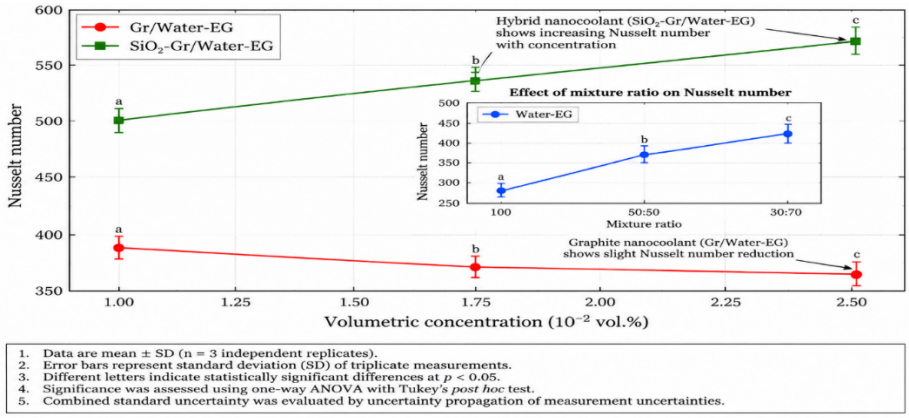


Figure 8. Effect of concentration on Nu for Water-EG, Gr/Water-EG, and SiO_2-Gr/Water-EG nanofluids.

4.7. Effect of Concentration on Thermal Conductivity Enhancement

Figure 9 shows the thermal conductivity enhancement of Gr/Water-EG and SiO_2-Gr/Water-EG nano-fluids as a function of nanoparticle volumetric fraction. Enhancement is evaluated relative to the Water-EG base fluid, with the figure showing a clear concentration-dependent improvement in thermal conductivity enhancement for both nanofluids, where the SiO_2-Gr/Water-EG hybrid nanofluid consistently outperformed the Gr/Water-EG nanofluid across the investigated nanoparticle volumetric fraction range. This progressive enhancement which increased with nanoparticle volumetric fraction for both nanofluid systems, confirms that particle loading improves conductive heat-transfer potential. For Graphite/Water-EG, the enhancement rises from approximately 0.02% at 1.0×10^{-2} to about 0.10% at 4.5×10^{-2}, indicating a near-linear improvement with concentration. The SiO_2-Gr/Water-EG hybrid nanofluid exhibits a higher enhancement over the entire range, increasing from roughly 0.067% to 0.13%. This superior response suggests that hybridization promotes a more effective thermal transport pathway than single-particle graphite dispersion, likely due to the complementary contribution of SiO_2 and graphite particles to energy transport within the base fluid.

Overall, the trend is important because the hybrid nanofluid maintains a consistent performance benefit at all concentrations. The difference between both fluids is more pronounced at lower particle fractions and becomes narrower at the highest concentration, where the Gr/Water-EG nanofluid approaches the hybrid nanofluid response. This indicates that increasing graphite loading improves conductivity substantially, while the hybrid formulation provides an earlier enhancement benefit even at lower concentration.

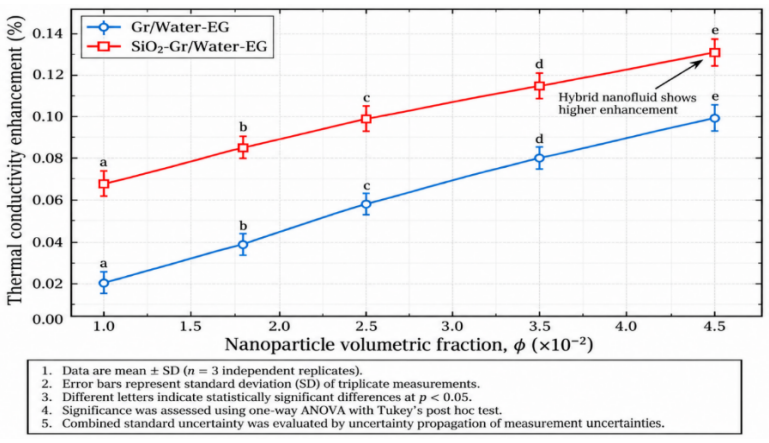
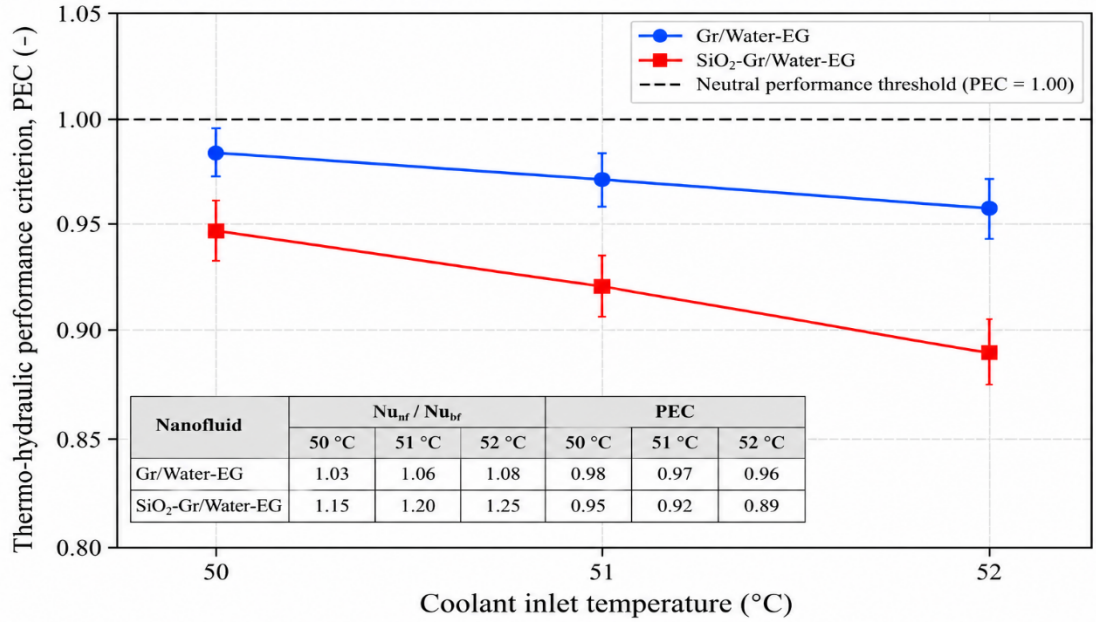


Figure 9. Impact of concentration on thermal Conductivity Enhancement (%) of Nanofluids.

4.8. Thermal–Hydraulic Performance Assessment: Heat-Transfer Enhancement Versus Hydraulic Penalty

Figure 10 presents the thermo-hydraulic performance criterion (PEC) of Gr/Water-EG and SiO_2-Gr/Water-EG nanofluids relative to the base fluid under different coolant inlet temperatures. The PEC values remained below unity for both nanofluids, indicating that the increase in heat-transfer capability was accompanied by a higher hydraulic penalty. Gr/Water-EG exhibited the closest approach to the neutral performance threshold (PEC = 1.0), demonstrating a more balanced thermal-hydraulic response, whereas SiO_2-Gr/Water-EG achieved higher Nusselt number enhancement but suffered a greater reduction in PEC due to increase in the estimated hydraulic penalty. These results highlight the importance of considering both heat-transfer enhancement and frictional losses when evaluating nanofluids for radiator applications.



Nanofluid	Nu_{nf} / Nu_{bf}			PEC		
	50 °C	51 °C	52 °C	50 °C	51 °C	52 °C
Gr/Water-EG	1.03	1.06	1.08	0.98	0.97	0.96
SiO_2-Gr/Water-EG	1.15	1.20	1.25	0.95	0.92	0.89

Figure 10. Thermo-hydraulic performance criterion of Gr/Water-EG and SiO_2-Gr/Water-EG nanofluids.

4.9. Enhancement Summary and Thermo-Hydraulic Assessment of Nanofluids

To provide a consolidated evaluation of the thermal and flow-performance characteristics of the investigated nanofluids, the maximum relative enhancements in thermal conductivity, Nusselt number, Reynolds number, viscosity variation, and thermo-hydraulic performance criterion (PEC) are summarised in Table 6. This summary complements the preceding graphical analyses by quantitatively comparing the performance of Gr/Water-EG and SiO_2-Gr/Water-EG nanofluids relative to the Water-EG base fluid.

The comparison demonstrates that nanoparticle hybridisation enhanced the thermal transport capability of the nanofluid system. The SiO_2-Gr/Water-EG hybrid nanofluid achieved the highest thermal conductivity enhancement (0.130%) and maximum Nusselt number enhancement (48.571%), compared with 0.099% and 17.714%, respectively, for Gr/Water-EG. The improved convective performance of the hybrid nanofluid can be attributed to the combined contribution of graphite and SiO_2 nanoparticles, which enhances energy transport pathways and modifies the thermo-physical behaviour of the base fluid.

The Reynolds number variation followed a similar trend, with the SiO_2-Gr/Water-EG nanofluid exhibiting a substantially higher relative increase (339.103%) compared with Gr/Water-EG (82.692%). However, this increase should not be interpreted independently as a direct measure of improved thermo-hydraulic performance because Reynolds number is influenced by changes in density, viscosity, and flow conditions. Therefore, the enhanced convective response must be evaluated together with the associated hydraulic penalty.

The viscosity analysis indicated only marginal changes across the investigated concentration range, with maximum increases of 0.085% for Gr/Water-EG and 0.055% for SiO_2-Gr/Water-EG. Although these variations are relatively small, the cumulative effect of modified thermophysical properties influences the frictional behaviour and must be considered when evaluating practical radiator applications. The conventional thermo-hydraulic performance criterion (PEC) was therefore considered to provide a more physically meaningful assessment by incorporating both heat-transfer enhancement and frictional effects. The estimated PEC values remained below unity for both nanofluids, indicating that the increase in heat-transfer capability was accompanied by an increase in hydraulic penalty. Gr/Water-EG exhibited PEC values of approximately 0.98, 0.97, and 0.96 at

50, 51, and 52 °C, respectively, demonstrating a comparatively balanced thermo-hydraulic response. In contrast, SiO_2-Gr/Water-EG achieved higher Nusselt number enhancement but showed lower PEC values of approximately 0.95, 0.92, and 0.89 over the same temperature range due to the greater relative hydraulic penalty.

Overall, the results demonstrate a trade-off between thermal enhancement and hydraulic performance. The SiO_2-Gr/Water-EG hybrid nanofluid is advantageous when maximum heat-transfer augmentation is prioritised, whereas Gr/Water-EG provides a more balanced thermo-hydraulic response with improved compatibility for applications where pumping requirements and energy consumption are critical considerations.

Table 6. Thermal enhancement, flow behaviour, and thermo-hydraulic performance comparison of nanofluids relative to base-fluid.

Performance Indicator	Gr/Water-EG	SiO_2-Gr/Water-EG	Comparative Basis
Maximum thermal conductivity enhancement (%)	0.099	0.130	Relative to Water-EG
Maximum Nusselt number enhancement (%)	17.714	48.571	Relative to Water-EG
Maximum Reynolds number variation (%)	82.692	339.103	Relative to Water-EG
Maximum viscosity increase (%)	0.085	0.055	Increase from lowest to highest tested concentration
PEC at 50 °C	0.98	0.95	Relative to Water-EG
PEC at 51 °C	0.97	0.92	Relative to Water-EG
PEC at 52 °C	0.96	0.89	Relative to Water-EG
Average PEC	0.97	0.92	Mean value across 50–52 °C

5. Conclusions

This study evaluated the thermophysical and convective heat-transfer behaviour of Water-EG, Gr/Water-EG and SiO_2-Gr/Water-EG fluids under varying concentration and inlet-temperature conditions. The findings show that nanoparticle addition enhanced thermal performance, but the improvement is governed by the balance between conductivity gain, viscosity rise and flow-response behaviour.

- Increasing nanoparticle volumetric fraction improved the thermal conductivity of both Gr/Water-EG and SiO_2-Gr/Water-EG nanofluids, confirming the positive contribution of dispersed nanoparticles to heat conduction. In contrast, increasing the EGC fraction in the Water-EG base fluid reduced thermal conductivity, indicating that EGC enrichment lowers the conductive heat-transfer potential of the base fluid. Viscosity increased with concentration for the base fluid and all nanofluids, showing the expected trade-off between thermal conductivity enhancement and flow resistance.
- The fluid-side Nusselt number increased with inlet temperature for the Water-EG base fluid and graphite/Water-EG nanofluid, indicating improved convective heat-transfer response at elevated inlet temperatures. However, the SiO_2-Gr/Water-EG nanofluid showed a decreasing Nusselt number with increasing inlet temperature, suggesting that the SiO_2-fortified suspension is more sensitive to temperature-induced changes in effective transport behaviour. Nevertheless, at 51 °C, the SiO_2-graphite nanofluid achieved a Nusselt number approximately 26% higher than the graphite nanofluid, demonstrating superior heat-transfer potential under the tested condition.
- Reynolds number increased with inlet temperature for the Water-EG and Gr/Water-EG fluid systems, indicating an increased tendency toward stronger inertial flow and enhanced convective transport. Conversely, the SiO_2-Gr/Water-EG nanofluid exhibited a reduction in Reynolds number with increasing inlet temperature, implying that SiO_2 addition modifies the flow response. Despite this, the SiO_2-Gr/Water-EG nanofluid maintained a Reynolds number 66.7% higher than the graphite nanofluid at 51 °C, confirming stronger flow activity at the selected operating point.
- With respect to nanoparticle volume fraction, the Nusselt number decreased for graphite/Water-EG but increased for SiO_2-Gr/Water-EG, indicating that hybridization improved concentration-dependent heat-transfer behaviour. The SiO_2-Gr/Water-EG nanofluid produced a Nusselt number 25.93% higher than the graphite-based (Gr) nanofluid, confirming that SiO_2 incorporation enhances the thermal response of the hybrid fluid, although its viscosity and Reynolds-number behaviour must be considered in practical radiator optimization.

Author Contributions

A.L.O.: conceptualization, methodology, software, supervision, validation; A.P.O.: data curation, methodology; writing—original draft preparation. All authors have read and agreed to the published version of the manuscript.

Funding

This research received no external funding.

Institutional Review Board Statement

Not applicable.

Informed Consent Statement

Not applicable.

Data Availability Statement

Data will be made available on request only to serious researchers.

Conflicts of Interest

The authors declare no conflict of interest.

Use of AI and AI-Assisted Technologies

No AI tools were utilized for this paper.

References

1. Yaw, C.T.; Koh, S.P.; Sandhya, M.; et al. Heat Transfer Enhancement by Hybrid Nano Additives—Graphene Nanoplatelets/Cellulose Nanocrystal for the Automobile Cooling System (Radiator). *Nanomaterials* **2023**, *13*, 808. https://doi.org/10.3390/nano13050808.
2. Harikrishnan, A.R.; Dhar, P.; Agnihotri, P.K.; et al. Effects of interplay of nanoparticles, surfactants and base fluid on the surface tension of nanocolloids. *Eur. Phys. J. E* **2017**, *40*, 1–31. https://doi.org/10.1140/epje/i2017-11541-5.
3. Hafeez, M.B.; Amin, R.; Nisar, K.S.; et al. Heat transfer enhancement through nanofluids with applications in automobile radiator. *Case Stud. Therm. Eng.* **2021**, *27*, 101192. https://doi.org/10.1016/j.csite.2021.101192.
4. Ardika, R.; Sudarno, S.; Winangun, K.; et al. The Effect of Using Variations of Radiator Fluid on the Effectiveness of Engine Cooling and the Rate of Corrosion of Radiator Materials in 1300 cc Cars. *Eng. Proc.* **2025**, *84*, 11. https://doi.org/10.3390/engproc2025084011.
5. Atanatizante. Ethylene Glycol and Engine Cooling. *F1technical.net*, January 25, 2020. Available online: https://www.f1technical.net/forum/viewtopic.php?t=28740 (accessed on 10 June 2024).
6. Tan, P.; Wang, P.; Fang, L.; et al. Exploring the performance of the thermal management system in a FCV based on real vehicle testing under different driving conditions. *Energy* **2025**, *336*, 138529. https://doi.org/10.1016/j.energy.2025.138529.
7. Dhumal, A.; Ambhore, N.; Kore, S.; et al. Investigation of the Effect of Different Fins Configurations on the Thermal Performance of the Radiator. *J. Adv. Res. Fluid Mech. Therm. Sci.* **2024**, *116*, 27–39. https://doi.org/10.37934/arfmts.116.1.2739.
8. Momin, M.; Atofarati, E.O.; Oladipo, S.; et al. Experimental characterization and predictive modelling of Al2O3/MWCNT hybrid nanofluid thermophysical properties using ANN, ANFIS, FCM and hybrid techniques. *J. Therm. Anal. Calorim.* **2026**, *151*, 11041–11071. https://doi.org/10.1007/s10973-026-15698-8.
9. Petinrin, M.O.; Ajuka, L.O.; Adebayo, A.S.; et al. Experimental Study of Flow and Heat Transfer in Rectangular Ducts with Ribbed Surfaces. In Proceedings of the International Conference on Innovative Academic Studies, Konya, Turkey, 10–13 September 2022.
10. Hussein, A.M.; Dawood, H.K.; Bakara, R.A.; et al. Numerical study on turbulent forced convective heat transfer using nanofluids TiO_2 in an automotive cooling system. *Case Stud. Therm. Eng.* **2017**, *9*, 72–78. https://doi.org/10.1016/j.csite.2016.11.005.
11. Ajuka, L.O.; Enweremadu, C.C. Comparative performance of liquid cooled micro/mini channel heat exchangers and macro-scale shell and tube exchangers in phase turbulent flow: A systematic review. *J. Therm. Anal. Calorim.* **2026**, 1–26. https://doi.org/10.1007/s10973-026-15538-9.
12. Oshionebo, F.D.; Kavaz, D.; Ozsahin, D.U.; et al. Optimized Nanofluid Fluids Enhance Thermal Performance in Ruffled Fin Automotive Radiators. *Sci. Rep.* **2025**, *15*, 43756. https://doi.org/10.1038/s41598-025-26764-w.
13. Yu, W.; Xie, H. A Review on Nanofluids: Preparation, Stability Mechanisms, and Applications. *J. Nanomater.* **2012**, *2012*, 435873. https://doi.org/10.1155/2012/435873.

14. Alami, A.H.; Ramadan, M.; Tawalbeh, M.; et al. A critical insight on nanofluids for heat transfer enhancement. *Sci. Rep.* **2023**, *13*, 15303. https://doi.org/10.1038/s41598-023-42489-0.
15. Wakif, A.; Chamkha, A.; Thumma, T.; et al. Thermal radiation and surface roughness effects on the thermo-magneto-hydrodynamic stability of alumina–copper oxide hybrid nanofluids utilizing the generalized Buongiorno's nanofluid model. *J. Therm. Anal. Calorim.* **2021**, *143*, 1201–1220. https://doi.org/10.1007/s10973-020-09488-z.
16. Chiam, H.W.; Azmi, W.H.; Usri, N.A.; et al. Thermal conductivity and viscosity of Al_2O_3 nanofluids for different based ratio of water and ethylene glycol mixture. *Exp. Therm. Fluid Sci.* **2017**, *81*, 420–429. https://doi.org/10.1016/j.expthermflusci.2016.09.013.
17. Levin, M.L.; Miller, M.A. Maxwell's Treatise on Electricity and Magnetism. *Sov. Phys. Uspekhi* **1981**, *24*, 904–913.
18. Rasool, G.; Wakif, A. Numerical spectral examination of EMHD mixed convective flow of second-grade nanofluid towards a vertical Riga plate using an advanced version of the revised Buongiorno's nanofluid model. *J. Therm. Anal. Calorim.* **2021**, *143*, 2379–2393. https://doi.org/10.1007/s10973-020-09865-8.
19. Soltani, F.; Toghraie, D.; Karimipour, A. Experimental measurements of thermal conductivity of engine oil-based hybrid and mono nanofluids with tungsten oxide (WO_3) and MWCNTs inclusions. *Powder Technol.* **2020**, *371*, 37–44. https://doi.org/10.1016/j.powtec.2020.05.059.
20. Esapour, M.; Hamzehnezhad, A.; Rabienataj Darzi, A.A.; et al. Melting and solidification of PCM embedded in porous metal foam in horizontal multi-tube heat storage system. *Energy Convers. Manag.* **2018**, *171*, 398–410. https://doi.org/10.1016/j.enconman.2018.05.086.
21. Jamshed, W.; Nisar, K.S.; Ibrahim, R.W.; et al. Computational frame work of Cattaneo-Christov heat flux effects on Engine Oil based Williamson hybrid nanofluids: A thermal case study. *Case Stud. Therm. Eng.* **2021**, *26*, 101179. https://doi.org/10.1016/j.csite.2021.101179.
22. Sathish, T.; Giri, J.; Saravanan, R.; et al. Amplifying thermal performance of solar flat plate collector by Al_2O_3/Cu/MWCNT/SiO_2 mono and hybrid nanofluid. *Appl. Therm. Eng.* **2024**, *252*, 123692. https://doi.org/10.1016/j.applthermaleng.2024.123692.
23. Shi, X.; Li, S.; Wei, Y.; et al. Numerical investigation of laminar convective heat transfer and pressure drop of water-based Al_2O_3 nanofluids in a microchannel. *Int. Commun. Heat Mass Transf.* **2018**, *90*, 111–120. https://doi.org/10.1016/j.icheatmasstransfer.2017.11.007.
24. Tumane, A.; Yewalikar, V.A.; Kubde, R.A.; et al. Experimental Analysis of Heat Transfer Enhancement of Car Radiator Using Cu Nanofluid with Base Fluid Water. *Int. Res. J. Mod. Eng. Technol. Sci.* **2023**, *5*, 3837–3846.
25. Asokan, N.; Gunnasegaran, P.; Wanatasanappan, V. Experimental investigation on the thermal performance of compact heat exchanger and the rheological properties of low concentration mono and hybrid nanofluids containing Al_2O_3 and CuO nanoparticles. *Therm. Sci. Eng. Prog.* **2020**, *20*, 100727. https://doi.org/10.1016/j.tsep.2020.100727.
26. Ramadhan, A.I.; Diniardi, E.; Basri, H.; et al. Experimental investigation of thermal conductivity of Al_2O_3-TiO_2-SiO_2 nanofluids in EG/water mixture for automotive radiator cooling system. In Proceedings of the 3RD International Conference of Bio-Based Economy for Application and Utility, Padang, Indonesia, 2023; Volume 2706, p. 020007. https://doi.org/10.1063/5.0120209.
27. Arbak, A.; Attar, A.; Altikatoglu Yapaoz, M.; et al. Experimental investigation of bimetallic nanoparticles heat transfer characteristics in automotive radiators. *Case Stud. Therm. Eng.* **2023**, *43*, 102763. https://doi.org/10.1016/j.csite.2023.102763.
28. Ukueje, W.E.; Abam, F.I.; Obi, A. A Perspective Review on Thermal Conductivity of Hybrid Nanofluids and Their Application in Automobile Radiator Cooling. *J. Nanotechnol.* **2022**, *2022*, 1–51. https://doi.org/10.1155/2022/2187932.
29. Cardenas Contreras, E.M.; Bandarra Filho, E.P. Heat transfer performance of an automotive radiator with MWCNT nanofluid cooling in a high operating temperature range. *Appl. Therm. Eng.* **2022**, *207*, 118149. https://doi.org/10.1016/j.applthermaleng.2022.118149.
30. Ramji, K.S.H.; Kumar, J.V.; Karthik, A.A. Experimental Investigation of Automobile radiator using Tungsten trioxide Nano-fluid. *IOP Conf. Ser. Mater. Sci. Eng.* **2020**, *995*, 012017. https://doi.org/10.1088/1757-899x/995/1/012017.
31. Erkan, A.; Tüccar, G.; Tosun, E.; et al. Comparison of effects of nanofluid utilization (Al_2O_3, SiO_2, TiO_2) with reference water in automotive radiators on exergetic properties of diesel engines. *SN Appl. Sci.* **2021**, *3*, 1–13. https://doi.org/10.1007/s42452-021-04368-z.
32. Vele, N.S.; Patil, R.K. Review on Heat Transfer Enhancement in Car Radiator Using Nanofluids. In Proceedings of the International Conference on Industrial Engineering and Operations Management, Bangkok, Thailand, 5–7 March 2019; pp. 527–537.
33. Kanti, P.K.; Marulasiddeshi, H.B.; Said, N.M.; et al. Bayesian-optimized machine learning and experimental study of Al_2O_3-CuO hybrid nanofluid thermal performance in turbulent circular tube flow. *Sci. Rep.* **2025**, *15*, 38717. https://doi.org/10.1038/s41598-025-23785-3.

34. Ajuka, L.O.; Ikumapayi, O.M.; Akinlabi, E.T. Entropy Generation of Graphene Nanoplatelets in Micro and Mini Channels: Nanofluid Flow in Automotive Cooling Applications. *Int. J. Heat Technol.* **2022**, *40*, 917–926. https://doi.org/10.18280/ijht.400408.
35. Kanti, P.K.; Marulasiddeshi, H.B.; Said, N.M.; et al. Experimental investigation of solar collector efficiency enhancement using surfactant stabilized MWCNT and Al_2O_3 hybrid nanofluid. *Sci. Rep.* **2026**, *16*, 17354. https://doi.org/10.1038/s41598-026-42016-x.
36. Choi, S.U.S.; Eastman, J.A. Enhancing Thermal Conductivity of Fluids with Nanoparticles. In Proceedings of the ASME International Mechanical Engineering Congress and Exposition, San Francisco, CA, USA, 12–17 November 1995, pp. 99–105. https://doi.org/10.1115/IMECE1995-0926.
37. Razzaq, I.; Xinhua, W.; Rasool, G.; et al. Nanofluids for Advanced Applications: A Comprehensive Review on Preparation Methods, Properties, and Environmental Impact. *ACS Omega* **2025**, *10*, 5251–5282. https://doi.org/10.1021/acsomega.4c10143.
38. Induranga, A.; Galpaya, C.; Vithanage, V.; et al. Nanofluids for Heat Transfer: Advances in Thermo-Physical Properties, Theoretical Insights, and Engineering Applications. *Energies* **2025**, *18*, 1935. https://doi.org/10.3390/en18081935.
39. Nature Index. Nanofluid Heat Transfer Dynamics and Thermophysical Properties. *Nature Index Topic Explorer, 2026*. Available online: https://www.nature.com/nature-index/topics/l4/nanofluid-heat-transfer-dynamics-and-thermophysical-properties (accessed on 11 August 2026).
40. Selvam, C.; Solaimalai Raja, R.; Mohan Lal, D.; et al. Overall heat transfer coefficient improvement of an automobile radiator with graphene based suspensions. *Int. J. Heat Mass Transf.* **2017**, *115*, 580–588. https://doi.org/10.1016/j.ijheatmasstransfer.2017.08.071.
41. Prasanna Shankara, R.; Banapurmath, N.R.; D'Souza, A.; et al. An insight into the performance of radiator system using ethylene glycol-water based graphene oxide nanofluids. *Alex. Eng. J.* **2022**, *61*, 5155–5167. https://doi.org/10.1016/j.aej.2021.10.037.
42. Abbas, F.; Ali, H.M.; Shaban, M.; et al. Towards convective heat transfer optimization in aluminum tube automotive radiators: Potential assessment of novel Fe_2O_3-TiO_2/water hybrid nanofluid. *J. Taiwan Inst. Chem. Eng.* **2021**, *124*, 424–436. https://doi.org/10.1016/j.jtice.2021.02.002.
43. Li, X.; Wang, H.; Luo, B. The thermophysical properties and enhanced heat transfer performance of SiC-MWCNTs hybrid nanofluids for car radiator system. *Colloids Surfaces A Physicochem. Eng. Asp.* **2021**, *612*, 125968. https://doi.org/10.1016/j.colsurfa.2020.125968.
44. Kumar, A.; Chand, P.; Hassan, M.A. Louvered finned car radiator with MWCNT-SiO_2 hybrid nanofluid: An experimental approach. *Powder Technol.* **2023**, *415*, 118176. https://doi.org/10.1016/j.powtec.2022.118176.
45. Hassaan, A.M. An experimental investigation examining the usage of a hybrid nanofluid in an automobile radiator. *Sci. Rep.* **2024**, *14*, 27597. https://doi.org/10.1038/s41598-024-78631-9.
46. Minh, C.N. Heat Transfer Enhancement Using Al_2O_3, CuO, and Hybrid Al_2O_3–CuO Nanofluids in Water and Ethylene Glycol–Water Mixtures in an Automotive Radiator. *Int. J. Heat Technol.* **2025**, *43*, 1429–1438. https://doi.org/10.18280/ijht.430420.